

Short communication

# Sodium ferrite $\text{Na}_2\text{O} \cdot 1.5\text{Fe}_2\text{O}_3$ as a high-capacity negative electrode for lithium-ion batteries

Shounan Hua<sup>a,\*</sup>, Gaoping Cao<sup>b</sup>, Yuezhi Cui<sup>a</sup>

<sup>a</sup> Department of Chemistry, Shandong University, Jinan, 250100, China

<sup>b</sup> Department of Applied Chemistry, Tianjin University, Tianjin, 300072, China

Received 28 May 1998; accepted 16 July 1998

## Abstract

Sodium ferrite,  $\text{Na}_2\text{O} \cdot 1.5\text{Fe}_2\text{O}_3$ , is studied as a novel active material for the negative electrodes of lithium-ion batteries. This material is prepared by decomposing a stoichiometric mixture of sodium carbonate and ferric oxide in air at 900°C for 24 h. The insertion and extraction of lithium ions is examined by means of a constant-current cycling technique and cyclic voltammetry using a  $\text{Li}/\text{Na}_2\text{O} \cdot 1.5\text{Fe}_2\text{O}_3$  cell. X-ray diffraction is used to examine the stability of the structure of the sodium ferrite electrodes during lithium insertion and extraction. The results show that the material has excellent cyclic performance and a high reversible capacity (360 mA h  $\text{g}^{-1}$ ) in a 1 M  $\text{LiClO}_4$  + PC electrolyte solution. © 1998 Elsevier Science S.A. All rights reserved.

**Keywords:** Sodium ferrite; Negative electrode material; Lithium-ion batteries; Lithium insertion

## 1. Introduction

Lithium intercalation compounds have been investigated as alternative negative-plate materials to lithium metal in rechargeable lithium batteries in order to overcome safety concerns and the short cycle life of secondary lithium metal batteries. Criteria for selecting such materials include: high reversible specific capacity, low electrode potential, small change in the chemical potential of the lithium ion in the material, high diffusion coefficient of lithium ions, compatibility with electrolyte and binders, dimensional and mechanical stability, safety in use, easy fabrication, etc. Carbon-based materials have been studied extensively as negative electrodes for lithium-ion batteries and rechargeable C/LiCoO<sub>2</sub> lithium-ion batteries have been commercialized for some portable devices. Although significant progress has been achieved in this area, the carbon materials cannot satisfy all conditions. It is therefore necessary to find better materials for rechargeable lithium-ion batteries. In recent years, there has emerged a great interest in transition metal oxides which offer a low

potential against pure lithium. The materials reported include: Fe<sub>2</sub>O<sub>3</sub> [1], WO<sub>2</sub>, MoO<sub>2</sub> [2], Nb<sub>2</sub>O<sub>5</sub> [3], Li<sub>4</sub>Ti<sub>5</sub>O<sub>12</sub>, Li<sub>4</sub>Mn<sub>5</sub>O<sub>12</sub>, Li<sub>12</sub>Mn<sub>4</sub>O<sub>9</sub> [4], TiO<sub>2</sub> [5], and CuCoS<sub>3</sub>O<sub>8</sub> [6]. They exhibit good rechargeability in PC-based electrolyte solutions, but their capacities are not satisfactory.

In this work, sodium ferrite with high reversible capacity has been prepared and a study has been made of its behaviour for lithium insertion and extraction.

## 2. Experimental

Sodium ferrite was synthesized from sodium carbonate (AR, Shanghai) and ferric oxide (AR, Shanghai) in air at 900°C for 24 h. The product had a brown colour and was powdered by controlled grinding and sieving using a 280 mesh standard screen. Chemical analysis confirmed the stoichiometry of the product to be  $\text{Na}_2\text{Fe}_3\text{O}_{5.5}$ . The X-ray diffraction pattern for this material is given in Fig. 1; this is in agreement with that of  $\text{Na}_2\text{O} \cdot 1.5\text{Fe}_2\text{O}_3$  reported in literature [7].

Charge–discharge cycling tests and chronopotentiometric experiments on  $\text{Na}_2\text{O} \cdot 1.5\text{Fe}_2\text{O}_3$  electrodes were performed in a three-electrode glass cell. The working electrode (1 × 1.5 cm) was made by mixing  $\text{Na}_2\text{O} \cdot 1.5\text{Fe}_2\text{O}_3$  powder with polytetrafluoroethylene (PTFE) and acetylene

\* Corresponding author. Tel.: +86-531-296-2917; Fax: +86-531-856-5167; E-mail: shua@jn-public.sd.cninfo.net

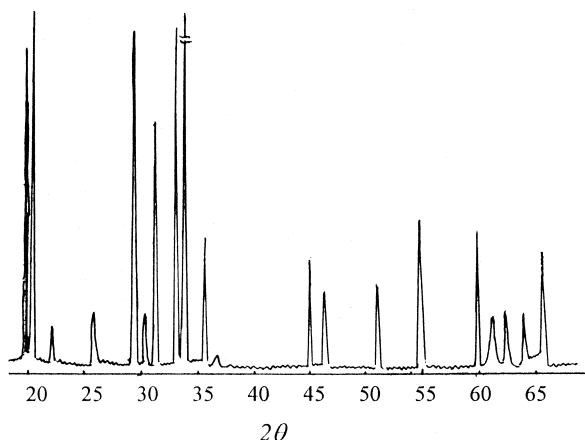


Fig. 1. X-ray diffraction pattern of  $\text{Na}_2\text{O} \cdot 1.5\text{Fe}_2\text{O}_3$ .

black in a mass ratio of 80:10:10, pressing the mixture on a nickel screen, and then drying at  $120^\circ\text{C}$  in air for at least 6 h. The loading of active material was  $20 \text{ mg cm}^{-2}$ . Lithium metal served as both the counter and the reference electrodes. The cell was assembled in a dry glove box and comprised a  $\text{Na}_2\text{O} \cdot 1.5\text{Fe}_2\text{O}_3$  electrode and two lithium electrodes separated with Celgard 2400 [8]. A tentative lithium-ion battery consisted of one  $\text{LiCoO}_2$  electrode and two  $\text{Na}_2\text{O} \cdot 1.5\text{Fe}_2\text{O}_3$  electrode. The electrolytes using in this work were PC containing 1 M  $\text{LiClO}_4$  or  $\text{LiAsF}_6$ , and PC + DEC (50:50, by volume) containing 1 M  $\text{LiClO}_4$  or  $\text{LiAsF}_6$ . The  $\text{LiAsF}_6$  (battery grade, Aldrich) was used without further treatment. The  $\text{LiClO}_4$  (AR, Shanghai) was dried at a temperature of 160 to  $180^\circ\text{C}$  and vacuum for 24 h prior to use. The solvents were dehydrated with a 4 Å molecular sieve for a week before being distilled.

The electrochemical behaviour of the electrodes was examined by means of a constant-current charge–discharge technique using an AMEL545 galvanostat–electrometer, and a cyclic voltammetric method using a HDV-7 potentiostat with a DCD-1 signal generator. X-ray diffraction measurements (D/Max-rA,  $\text{CuK}_\alpha$  radiation) were carried out ex situ on electrodes before and after cycling.

### 3. Results and discussion

Typical charge–discharge curves of a  $\text{Li}/\text{Na}_2\text{O} \cdot 1.5\text{Fe}_2\text{O}_3$  cell with a 1 M  $\text{LiClO}_4 + \text{PC}$  electrolyte are shown in Fig. 2. The current density is  $0.25 \text{ mA cm}^{-2}$ , and the voltage range is from 0.25 V for discharge to 2.5 V for charge. During the first discharge, the cell voltages decrease rapidly to 1.2 V, and then more slowly to 0.25 V. There are several plateaux on the first discharge curve, while subsequent discharge curves become smooth. The first and subsequent charge curves are smooth. The cycling efficiency on the first cycle is 51%, but then becomes approximately 100% on later cycles. The irreversible capacity of the cell is exhibited only during the first dis-

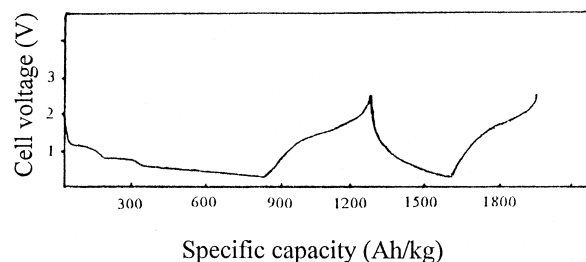


Fig. 2. First and second charge–discharge curves for  $\text{Li}/1 \text{ M LiClO}_4 + \text{PC}/\text{Na}_2\text{O} \cdot 1.5\text{Fe}_2\text{O}_3$  cell.

charge. This irreversible capacity is caused by two factors. The first relates to the reduction of solution species. It has been reported that a few electrolyte solutions, including PC, are reduced at potentials below 1.5 V vs.  $\text{Li}/\text{Li}^+$  at non-active metal or carbon electrodes to form a surface film called the ‘solid electrolyte interface’ (SEI) [9–12]. The film completely isolates the active mass from the solution before the electrode reaches the intercalation potential, then the electrodes are stabilized. We conclude that a similar reaction mechanism might be possible for the  $\text{Na}_2\text{O} \cdot 1.5\text{Fe}_2\text{O}_3$  electrode because it is polarized to a low potential during the first discharge. The second factor relates to lithium irreversibly remaining in the bulk of the  $\text{Na}_2\text{O} \cdot 1.5\text{Fe}_2\text{O}_3$  electrode material after the initial discharge.

Typical cyclic voltammograms for the  $\text{Na}_2\text{O} \cdot 1.5\text{Fe}_2\text{O}_3$  electrode in 1 M  $\text{LiClO}_4 + \text{PC}$  electrolyte are shown in Fig. 3. Five peaks at 1.60, 1.15, 0.90, 0.40 and 0.01 V vs.  $\text{Li}/\text{Li}^+$  are present in the first cathodic scan. In the reverse scan, only two anodic peaks at 0.15 and 1.50 V are observed. Two minor cathodic peaks at 1.15 and 0.90 V and no corresponding peaks in the following anodic curve are probably associated with the reduction of the elec-

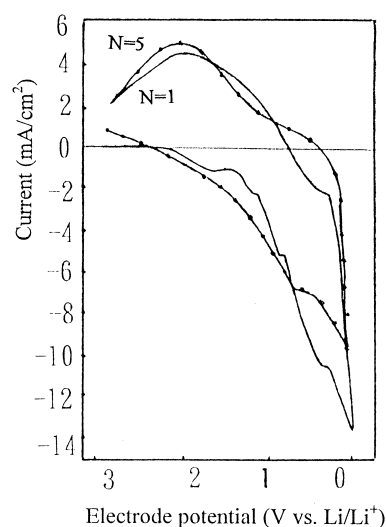


Fig. 3. Typical cyclic voltammograms for  $\text{Li}/1 \text{ M LiClO}_4 + \text{PC}/\text{Na}_2\text{O} \cdot 1.5\text{Fe}_2\text{O}_3$  cell. Scan rate:  $0.2 \text{ mV s}^{-1}$ .  $N$  = cycle number.

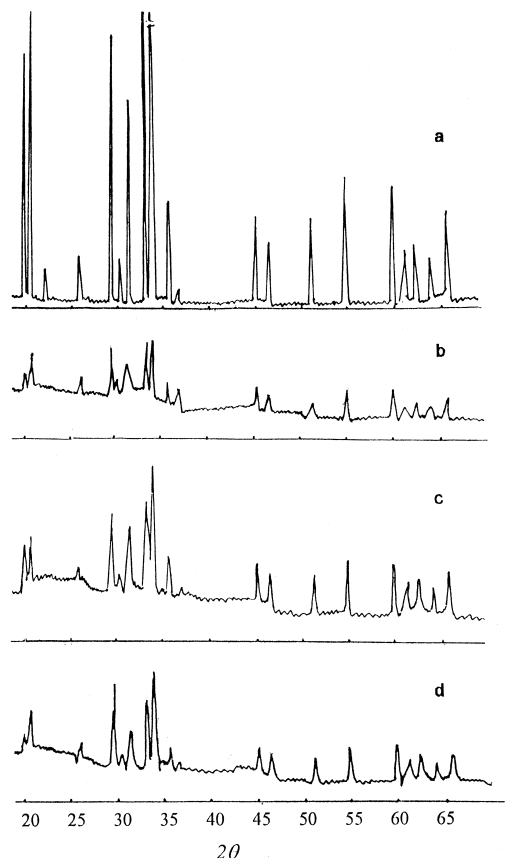


Fig. 4. X-ray diffraction patterns for  $\text{Na}_2\text{O} \cdot 1.5\text{Fe}_2\text{O}_3$  electrodes: (a) before cycling; (b) after the first discharge; (c) after the first charge; (d) after fifteenth charge.

trolyte on the surface of the negative electrode. This explanation is supported by the generation of bubbles from an excess electrolyte cell starting at 1.2 V and stopping at 0.8 V during the first negative-going scan. The peaks at 0.40 and 1.50 V correspond to the lithium intercalation and de-intercalation processes in the  $\text{Na}_2\text{O} \cdot 1.5\text{Fe}_2\text{O}_3$  host. The other two peaks (0.01 and 0.15 V) correspond to the deposition and stripping of metallic lithium on the electrode surface. After cycling, the three original cathodic peaks (at 1.60, 1.15 and 0.90 V) fade away. On the fifth cycle, one cathodic peak at potentials from 0.25 to 3.00 V remains; this agrees with the second discharge curve of Fig. 2. These results indicate that after cycling the side reactions, including electrolyte decomposition to form a surface film on the  $\text{Na}_2\text{O} \cdot 1.5\text{Fe}_2\text{O}_3$  electrode, are finished. The subsequent electrode reactions are mainly the reversible intercalation and deintercalation of lithium at the electrode, therefore, steady state behaviour approaches.

In order to examine the structural changes of electrodes during the charge and discharge processes, the X-ray diffraction patterns of the  $\text{Na}_2\text{O} \cdot 1.5\text{Fe}_2\text{O}_3$  electrodes before and after cycling in PC + 1 M  $\text{LiClO}_4$  are shown in Fig. 4. The charge–discharge current density is  $0.25 \text{ mA cm}^{-2}$ , and the potential range is between 0.25 and 2.5 V vs.  $\text{Li}/\text{Li}^+$ . As seen from Fig. 4(b), with the intercalation

of lithium ions into  $\text{Na}_2\text{O} \cdot 1.5\text{Fe}_2\text{O}_3$ , the diffraction peak at  $d = 3.991$  disappears and the relative intensities of the peaks at  $d = 4.457$ , 2.636 and 2.444 change. When lithium ions are withdrawn from the electrode, the changed peaks recover except for the  $d = 3.991$  peak, as seen in Fig. 4(c). This shows that the structural changes during the charge and discharge processes are recoverable. It is also observed that the diffraction pattern Fig. 4(d) for the sample after the 15th charge is very similar to that for the original charge Fig. 4(a). Thus, the structure of the material is stable for lithium insertion and extraction.

Discharge–charge curves for  $\text{Li}/\text{Na}_2\text{O} \cdot 1.5\text{Fe}_2\text{O}_3$  cells in different electrolytes at a current density of  $0.25 \text{ mA cm}^{-2}$  and over a voltage region of 0.25 to 2.5 V are presented in Fig. 5. The electrolytes used in this study are: 1 M  $\text{LiClO}_4$  + PC, 1 M  $\text{LiClO}_4$  + (PC + DME), 1 M  $\text{LiAsF}_6$  + PC and 1 M  $\text{LiAsF}_6$  + (PC + DME). As shown in Fig. 5, the performance of  $\text{Na}_2\text{O} \cdot 1.5\text{Fe}_2\text{O}_3$  electrodes in different electrolytes is very different. High specific capacity and long cycling life are obtained in 1 M  $\text{LiClO}_4$  + PC. The reversible capacity is very low in 1 M  $\text{LiClO}_4$  + (PC + DME). The strong influence of the electrolyte solution upon the charge–discharge behaviour of the  $\text{Na}_2\text{O} \cdot 1.5\text{Fe}_2\text{O}_3$  electrodes is probably related to the electrolyte decomposition during the first discharge and differences in the SEI on the electrodes in different electrolytes.

The charge and discharge curves of the tentative lithium-ion battery  $\text{Na}_2\text{O} \cdot 1.5\text{Fe}_2\text{O}_3/1 \text{ M LiClO}_4$  + PC/ $\text{LiCoO}_2$  are shown in Fig. 6. The current density is  $0.25 \text{ mA cm}^{-2}$  and the voltage range is 1.4 to 3.8 V. In order to compare the negative and positive electrode, the potentials of the two electrodes vs. lithium reference are

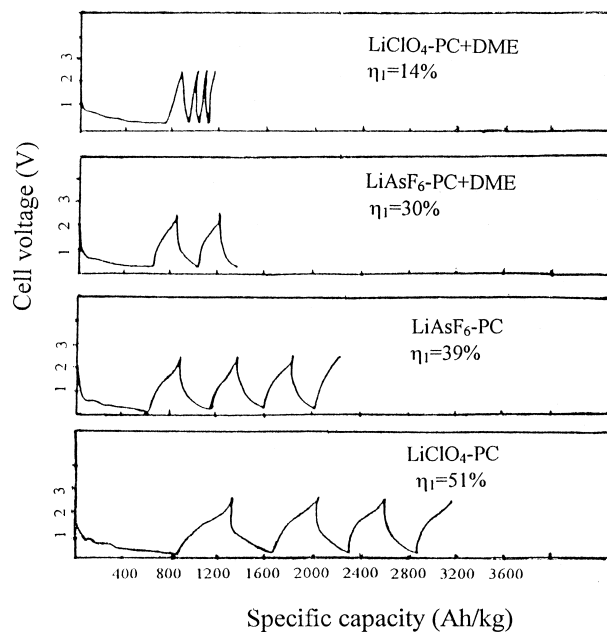


Fig. 5. Charge–discharge curves for  $\text{Li}/\text{Na}_2\text{O} \cdot 1.5\text{Fe}_2\text{O}_3$  cells in various electrolytes at a cycling current of  $0.25 \text{ mA cm}^{-2}$  ( $\eta_1$  = first cycling efficiency).

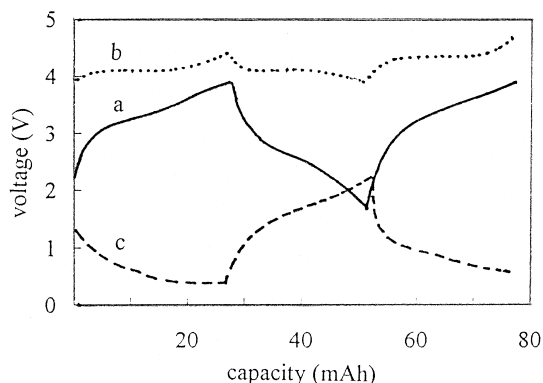


Fig. 6. Discharge–charge curves and potentials of electrodes for  $\text{Na}_2\text{O} \cdot 1.5\text{Fe}_2\text{O}_3 / 1 \text{ M LiClO}_4 + \text{PC} / \text{LiCoO}_2$  lithium-ion battery: (a) discharge–charge curves of battery; (b) potential of  $\text{LiCoO}_2$  electrode; (c) potential of  $\text{Na}_2\text{O} \cdot 1.5\text{Fe}_2\text{O}_3$  electrode.

also shown in Fig. 6. The average voltage of the battery is about 2.5 V. The change of cell voltage comes mainly from the  $\text{Na}_2\text{O} \cdot 1.5\text{Fe}_2\text{O}_3$  electrode.

#### 4. Conclusions

The sodium ferrite  $\text{Na}_2\text{O} \cdot 1.5\text{Fe}_2\text{O}_3$  electrode has a reversible specific capacity of up to  $360 \text{ mA h g}^{-1}$  for lithium insertion and exhibits good cycling performance in PC containing 1 M  $\text{LiClO}_4$ . X-ray analyses of charged and discharged samples reveal that the structure of the sodium ferrite is stable for lithium insertion and extraction. Thus, sodium ferrite  $\text{Na}_2\text{O} \cdot 1.5\text{Fe}_2\text{O}_3$  can be considered as a negative material for lithium-ion batteries. The  $\text{Na}_2\text{O} \cdot$

$1.5\text{Fe}_2\text{O}_3$  electrode displays irreversible capacity only on the first cycle. It is concluded that this irreversible capacity is probably due to electrolyte decomposition and to lithium irreversibly remaining in the  $\text{Na}_2\text{O} \cdot 1.5\text{Fe}_2\text{O}_3$  electrodes.

#### Acknowledgements

This work was supported by the National Natural Science Foundation of The People's Republic of China.

#### References

- [1] B. Di Pietro, M. Patriarca, B. Scrosati, *J. Power Sources* 8 (1982) 289.
- [2] J.J. Auborn, Y.L. Barbero, *J. Electrochem. Soc.* 134 (1987) 638.
- [3] Watanabe, Atsushi, Kato, Toshiyuki, *Jpn. Pat. Appl.*, 91/119, 321, 23 April 1991.
- [4] E. Ferg, J. Gummow, A. de Kock, M.M. Thackeray, *J. Electrochem. Soc.* 141 (1994) L147.
- [5] S.Y. Huang, L. Kavan, I. Exnar, M. Gratzel, *J. Electrochem. Soc.* 142 (1995) L142.
- [6] M.A. Cochez, J.C. Jumax, P. Lavela, J. Morales, J. Olivier-Fourcade, J.L. Tirado, *J. Power Sources* 62 (1996) 101.
- [7] P.J. Thery, R. Collongues, *Bull. Soc. Chem. France* 1959 (1959) 1141.
- [8] S.N. Hua, G.L. Zong, N.Z. Jiang, *J. Power Sources* 63 (1996) 93.
- [9] D. Aurbach, M. Daroux, P. Faguy, E.B. Yeager, *J. Electrochem. Soc.* 134 (1987) 1611.
- [10] D. Aurbach, H. Gottlieb, *Electrochem. Acta* 34 (1989) 141.
- [11] R. Fong, U. Von Sackon, J.R. Dahn, *J. Electrochem. Soc.* 137 (1990) 2009.
- [12] Y. Matsumura, S. Wang, J. Mondori, *J. Electrochem. Soc.* 142 (1995) 2914.